Model for Adsorption of Ligands to Colloidal Quantum Dots with Concentration-Dependent Surface Structure

Adam J. Morris-Cohen, Vladislav Vasilenko, Victor A. Amin, Matthew G. Reuter, and Emily A. Weiss*

Department of Chemistry, Northwestern University, 2145 Sheridan Road, Evanston, Illinois 60208-3113, United States

ABSTRACT

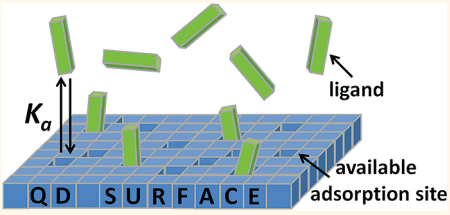

A study of the adsorption equilibrium of solution-phase CdS quantum dots (QDs) and acid-derivatized viologen ligands (*N*-[1-heptyl],*N*′-[3-carboxypropyl]-4,4′-bipyridinium dihexafluorophosphate, V^{2+}) reveals that the structure of the surfaces of the QDs depends on their concentration. This adsorption equilibrium is monitored through quenching of the photoluminescence of the QDs by V^{2+} upon photoinduced electron transfer. When modeled with a simple Langmuir isotherm, the equilibrium constant for QD—V^{2+} adsorption, K_a, increases from 6.7×10^5 to 8.6×10^6 M^{-1} upon decreasing the absolute concentration of the QDs from 1.4×10^{-6} to 5.1×10^{-8} M. The apparent increase in K_a upon dilution results from an increase in the mean number of available adsorption sites per QD from 1.1 (for [QD] = 1.4×10^{-6} M) to 37 (for [QD] = 5.1×10^{-8} M) through desorption of native ligands from the surfaces of the QDs and through disaggregation of soluble QD clusters. A new model based on the Langmuir isotherm that treats both the number of adsorbed ligands per QD and the number of available binding sites per QD as binomially distributed quantities is described. This model yields a concentration-independent value for K_a of 8.7×10^5 M^{-1} for the QD—V^{2+} system and provides a convenient means for quantitative analysis of QD—ligand adsorption in the presence of competing surface processes.

KEYWORDS: quantum dot · binomial distribution · ligand adsorption · equilibrium constant · photoluminescence

This paper describes a study of the adsorption equilibrium of a solution-phase system of CdS quantum dots (QDs) and acid-derivatized viologen ligands (*N*-[1-heptyl],*N*′-[3-carboxypropyl]-4,4′-bipyridinium dihexafluorophosphate, V^{2+}, Figure 1A) as a function of the concentration of QDs. We observe that the QD—V^{2+} adsorption constant (K_a), when determined by fitting adsorption data with a simple Langmuir isotherm, changes with the absolute concentration of QDs; the concentration dependence of K_a results from a dilution-induced increase in the average number of available surface sites on each QD to which V^{2+} can adsorb. We demonstrate that modeling the QD—V^{2+} adsorption equilibrium with a modified Langmuir isotherm that explicitly treats both the number of adsorbed V^{2+} per QD and the number of available binding sites per QD as binomially distributed quantities yields a single, concentration-independent value of K_a and enables quantitative characterization of the surface sites on the QD.

Quantum-dot-based materials are potentially useful in several applications, including sensors and photovoltaics, that require generation of photocurrent from the excited state of the QD.[1] The rate of electron transfer across the interface between the QD core and the surrounding medium is an important parameter in determining the efficiency of photocurrent generation. We have shown in a recent publication on electron transfer within solid-state QD—poly(viologen) mixtures[2] that the ability of poly(viologen) to position itself within tunneling distance of the QD core in the presence of an adlayer of native ligands on the QD determines the rate of charge separation in nanostructured donor—acceptor films. The intermolecular structure of the native ligand adlayer is determined by the chemical structure and concentration of native ligands on the surface of the QD. The model we present here is therefore relevant to applications requiring charge separation in QD-based materials because it enables quantitative characterization of the composition of the mixed layer of native and redox-active ligands on the surfaces of the QDs.

* Address correspondence to e-weiss@northwestern.edu.

Received for review October 13, 2011 and accepted December 1, 2011.

Published online December 01, 2011
10.1021/nn203950s

Our analysis of QD−ligand binding equilibria has two major advantages over previous similar studies: (i) Previous measurements of K_a for QD−ligand complexes have assumed some relationship (often linear) between the photoluminescence (PL) intensity of the QD ensemble and the surface coverage of a PL quenching ligand[3−6] but have not measured this relationship directly. We use a ligand, V^{2+}, for which we know the relationship between PL of the QD and surface coverage of the ligand from previous PL and transient absorption studies of photoinduced electron transfer from the QD to V^{2+}.[7] Knowledge of the PL response of the QDs to adsorbed V^{2+} allows us to relate directly the PL intensity to the distribution of V^{2+} adsorbed to the QDs. (ii) Unlike previous applications of the basic Langmuir isotherm to QD−ligand systems,[3,4,6,8−11] our model enables quantitative determination of K_a for QD−ligand complexes in the presence of competing processes that alter the availability of binding sites without assumptions about or direct measurements of the strength or nature of these competing processes. We group together all processes that remove potential V^{2+} adsorption sites and characterize the remaining sites as "available surface sites". Our model allows us to quantitatively determine changes in the surface coverage of QDs upon dilution and, in doing so, reveals a highly competitive environment at the surface of the QD with few surface sites available to adsorbing ligands.

Below, we describe how we relate the PL of the QDs to the distribution of adsorbed V^{2+} in the ensemble. We then analyze the QD−V^{2+} adsorption data using a simple Langmuir isotherm and demonstrate that this approach is insufficient because it yields values of K_a for the QD−V^{2+} complex that depend on the concentration of QDs. We derive a new model for the QD−V^{2+} adsorption equilibrium that accounts for the changing number of available surface sites on the QD with dilution and use this model to obtain a single, concentration-independent value of K_a and the distribution of available adsorption sites per QD at each concentration.

RESULTS AND DISCUSSION

Synthesis and Purification of CdS QDs and V^{2+}. We synthesized *N*-[1-heptyl],*N*′-[3-carboxypropyl]-4,4′-bipyridinium dihexafluorophosphate (V^{2+}) by a procedure published previously.[7] We synthesized CdS QDs with a procedure adapted from Yu and Peng.[12] In a three-neck round-bottom flask, we heated 42.6 mg of CdO, 14.7 mL of octadecene (ODE), and 0.3 mL of oleic acid to 300 °C under nitrogen and, once the CdO was completely dissolved, swiftly injected 1 mL of freshly prepared 0.15 M sulfur in ODE and allowed it to react at 250 °C. After 1 h, we made two dropwise additions of sulfur precursor (1 and 0.5 mL, 1 drop/s, 10 min apart). After 5 min of growth, we cooled the reaction mixture to 90 °C, kept the mixture at that temperature for 2 h, and then cooled the mixture to room temperature. Once the reaction mixture cooled, we purified the QDs by extraction with a mixture of methanol and chloroform (1:1:2, methanol/chloroform/octadecene). After decanting the methanol/chloroform fraction, we added another 5 mL of chloroform and enough acetone to precipitate the QDs. Centrifugation and decantation separated the QDs from the supernate. We resuspended the pellet in chloroform to create a solution with an optical density of 1 in a 1 cm cuvette at the first excitonic peak (425 nm).

Optical Properties of the CdS QDs. The absorption spectrum of the QDs (Figure 1B, black) has a first excitonic peak at 425 nm, which corresponds to a diameter of 4.3 nm.[13] The photoluminescence (PL) spectrum of the QDs (Figure 1B, red) shows a strong, broad emission band centered at 610 nm with a line width (fwhm) of 150 nm, which we assign to deep-trap emission, and a weak band at 454 nm, which we assign to band-edge emission. The excess sulfur used in the synthesis and the predominance of deep-trap emission in the PL spectrum suggest that these oleate-capped QDs have unpassivated sulfur atoms on the surface that act as emissive hole traps.[14]

Preparation of QD−V^{2+} Samples. We prepared four series of CdS QD−V^{2+} solutions: D0, D1, D2, and D3. Each series of samples contained a different concentration of QDs. We prepared the D0 series by adding 75 μL of a stock solution of V^{2+} in acetonitrile (ACN) at an appropriate concentration to equimolar, equivolume solutions of QDs in $CHCl_3$ so that the final solutions were 1.4×10^{-6} M in CdS QDs and had molar ratios V^{2+}/QD equal to 0, 0.19, 0.38, 0.76, 1.5, 3.1, 6.1, 12, 24, and 49. The resulting solutions were all 40:1 $CHCl_3$/ACN. We prepared the D1 series by diluting all of the samples in the D0 series by a factor of 3 with 40:1 $CHCl_3$/ACN. The D2 and D3 series were similarly prepared by 3-fold dilutions of D1 and D2, respectively. We allowed all of the solutions to equilibrate for 1 day in the dark prior to measuring their PL spectra.

Magnitude of QD PL Reveals the Fraction of QDs with Zero Adsorbed V^{2+}. To determine the QD−V^{2+} adsorption constant, we measured the PL intensity of solutions of CdS QDs with oleate native ligands as a function of the added concentration of V^{2+}. We collected the emission spectra of samples in a 1 cm quartz cuvette on a Fluorolog-3 spectrofluorimeter (Horiba JobinYvon Spex) with an excitation wavelength λ_{exc} = 400 nm over a range of 405−800 nm. The emission and excitation slit widths were set to pass an effective bandwidth of 4 nm. The magnitude of the PL was calculated by doubling the integrated emission from the emission maximum at 610−800 nm (half the emission peak); we thereby avoided a small convoluting signal present in the D2 and D3 samples at high concentration of V^{2+} (see Supporting Information).

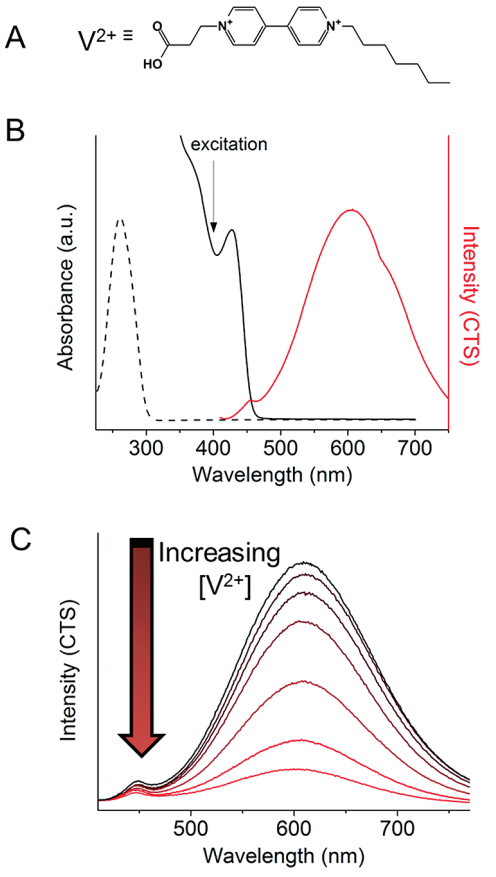

Figure 1. (A) Chemical structure of *N*-[1-heptyl],*N*′-[3-carboxypropyl]-4,4′-bipyridinium (V^{2+}). (B) Absorbance (black, solid) and emission (red, solid) spectra of 1.4×10^{-6} M, 4.3 nm diameter CdS QDs in 40:1 $CHCl_3$/ACN and absorbance spectrum of V^{2+} (black, dashed). We calculate the emission intensity by doubling the integrated emission of the QDs from the emission maximum at 610−800 nm. (C) PL spectra of 1.4×10^{-6} M, 4.3 nm diameter CdS QDs in 40:1 $CHCl_3$/ACN after excitation at 400 nm with increasing concentrations of added V^{2+}. The range of molar ratios V^{2+}:QD represented in this plot is 0.2:1 (highest PL trace, black) to 12.5:1 (lowest PL trace, red).

We believe, but have not yet proven, that this "extra" emission peak (which was not used in the analysis described here) originates from charge recombination of the QD^+-V^+ state to form $QD-V^{2+}$. We are currently investigating the nature of this signal in more detail.

For each of the four series D0−D3, increasing the concentration of V^{2+} decreases the PL intensity of the QDs (Figure 1C). We have shown previously[7] that V^{2+} quenches the PL of CdS QDs through photoinduced electron transfer (PET) with an "intrinsic" (single donor−single acceptor) rate constant of 1.7×10^{10} s^{-1} ($\tau = 59$ ps) in a mixture of dichloromethane/ACN (33:1 by volume). In that work, we showed that (i) the PL of a QD with one or more adsorbed V^{2+} molecules is completely quenched because the PET rate constant is ~1000 times larger than the rate constant for radiative recombination of the QD exciton, and (ii) the formation of the QD−ligand complex is a stochastic process resulting in a distribution of the number of adsorbed ligands per QD.[15] Given the quantitative quenching by a single adsorbed V^{2+}, the decrease in PL intensity of the ensemble of QDs with increasing concentration of V^{2+} must result from a decrease in the concentration of QDs with zero adsorbed V^{2+}. We therefore interpret PL/PL_0, defined as the ratio of the integrated PL intensity after addition of V^{2+} to the integrated intensity before the addition of V^{2+}, as the fraction of QDs within the ensemble that have zero adsorbed V^{2+}.[7] The ensemble is completely quenched when the concentration of QDs with zero adsorbed V^{2+} is below the limit of PL detection.

The Binomial Distribution Relates the Fraction of QDs with Zero Adsorbed V^{2+} to the Mean Number of Adsorbed V^{2+} per QD. Both the Poisson[16] and binomial[17] distributions describe the statistics of uncorrelated adsorption of ligands to QD surfaces. If (i) the mean number of surface-bound ligands is far from the number needed to saturate the QD surface, and (ii) there is a sufficiently large number of surface sites, the distribution of ligands can be described equivalently by either a Poisson distribution or a binomial distribution. When the number of ligands adsorbed to the surface of the QD approaches saturation, however, the Poisson distribution predicts a non-negligible probability that a QD will contain more ligands than there are adsorption sites. In this case, the Poisson distribution becomes nonphysical and the binomial distribution must be used.[17,18] Previously,[7] we used the Poisson distribution to describe the adsorption equilibrium of V^{2+} ligands on CdS QDs and to calculate the intrinsic (single donor−single acceptor) rate constant, k_{int}, of charge transfer from a photoexcited CdS QD to V^{2+}. Although we collected some of our data near the saturation limit in this study, re-analysis of the total data set using a binomial distribution shows that, for that particular case, the value k_{int} does not change compared to the values obtained when using the Poisson distribution (see Supporting Information).

Here, following previous work in heterogeneous micellar systems,[17] we use the more generally applicable binomial distribution to relate the fraction of QDs that have zero adsorbed V^{2+} to the mean fractional surface coverage of V^{2+} on the QDs in the ensemble. The binomial distribution (eq 1) gives the probability of finding a QD with m adsorbed V^{2+} ligands, given that

$$P(m\,|\,N,\theta) = \binom{N}{m}(\theta)^m(1-\theta)^{N-m} \qquad (1)$$

N is the total number of surface sites per QD and θ is the mean fractional surface coverage of V^{2+} on the QDs in the ensemble. Table 1 lists the definitions of all of the parameters used in this paper. We estimate N to be 410 from the surface area of the QD.[5] The probability of finding a QD with zero adsorbed ligands, $P(0|N,\theta)$, equals the experimentally measured fraction of original PL

TABLE 1. Definitions and Methods of Determination of the Parameters Used in This Study

parameter	definition	method of determination
N	total number of surface sites per QD, here 410	calculated from surface area of QD
n	number of available surface sites on a QD[a]	probability is given by the binomial distribution and η
η	$\langle n \rangle$	fit parameter in eq *10*
m	number of V^{2+} adsorbed to a QD[a]	probability is given by the binomial distribution and θ_a
θ	mean fractional surface coverage of total sites by V^{2+}. $\langle m \rangle / N$	calculated using eq *2*
θ_a	mean fractional surface coverage of available sites by V^{2+}. $\langle m \rangle / \eta$	implicit parameter in eq *10*
θ_{max}	maximum fractional surface coverage of total sites	fit parameter in eq *4*; suggests necessity of η
K_a	adsorption constant	fit parameter in eqs *4* and *10*
$[V^{2+}]_{total}$	total concentration of viologen in sample	measured when preparing sample
$[V^{2+}]_{free}$	concentration of viologen not bound to a QD	calculated using eq *3*
$P_{ligands}$	probability to find m ligands on a QD	calculated using eq *6*
P_{sites}	probability to find n available surface sites	calculated using eq *5*

[a] Indicates a microscopic quantity.

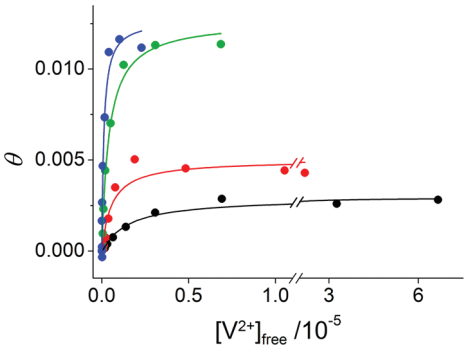

Figure 2. Mean fractional surface coverage of V^{2+} on the QDs (θ) as a function of the concentration of free V^{2+} for samples of 1.4×10^{-6} M CdS QDs (D0, black), 4.6×10^{-7} M CdS QDs (D1, red), 1.5×10^{-7} M CdS QDs (D2, green), and 5.1×10^{-8} M CdS QDs (D3, blue). The solid lines are best-fits using a simple Langmuir isotherm (eq 4).

intensity that remains after addition of V^{2+} (PL/PL_0) (eq 2). Equation 2 also gives the relationship between the

$$P(0|N,\theta) = \frac{PL}{PL_0} = (1-\theta)^N \qquad (2)$$

measured quantity PL/PL_0 and θ. Figure 2 shows plots of θ (calculated using eq 2) *versus* the concentration of free V^{2+} for the series D0–D3. Notice that in Figure 2 the independent variable is $[V^{2+}]_{free}$, as calculated using eq 3, not $[V^{2+}]_{total}$.

$$[V^{2+}]_{free} = [V^{2+}]_{total} - [V^{2+}]_{bound} = [V^{2+}]_{total} - [QD]N\theta \qquad (3)$$

Simple Langmuir Model Yields a Concentration-Dependent Equilibrium Constant. We fit the data in Figure 2 to the Langmuir isotherm (eq 4). To obtain a satisfactory fit of

$$\theta = \theta_{max}\frac{K_a[V^{2+}]_{free}}{1+K_a[V^{2+}]_{free}} \qquad (4)$$

the data with eq 4, we need to include the parameter θ_{max}, the fractional surface coverage of V^{2+} on the QD

TABLE 2. Comparison of the Best-Fit Values for K_a and θ_{max} Using the Simple Langmuir Isotherm (eq 4) and the Global Fit Based on the Double Binomial Distribution Model (eq 10) for All Four Concentrations of QDs (Also Shown Are the Mean Numbers of Empty Sites, η, Predicted from the Double Binomial Distribution Model)

		simple Langmuir (eq *3*)		double binomial (eq *10*)	
sample	[QD][a]	K_a (M^{-1})	θ_{max}	K_a (M^{-1})	η
D0	1.4×10^{-6}	6.7×10^5	0.003	8.7×10^5	1.1
D1	4.6×10^{-7}	1.8×10^6	0.005	8.7×10^5	2.5
D2	1.5×10^{-7}	2.4×10^6	0.01	8.7×10^5	9.6
D3	5.1×10^{-8}	8.6×10^6	0.01	8.7×10^5	37

[a] Calculated from the ICP-AES as described in the Supporting Information.

at which θ saturates; the need for this parameter indicates that there are fewer surface sites available to V^{2+} than the 410 we estimated from the surface area of a bare QD—that is, not all surface sites are available to adsorbing molecules.

From the fits of the data in Figure 2 to eq 4, we extract a value for the QD–V^{2+} adsorption constant, K_a, at each concentration of QDs (D0–D3). The value of K_a we obtain from the Langmuir fits to the data in Figure 2 increases from 6.7×10^5 M^{-1} for $[QD] = 1.4 \times 10^{-6}$ M (D0) to 8.6×10^6 M^{-1} for $[QD] = 5.1 \times 10^{-8}$ M QDs (D3), while the value of θ_{max} increases from 0.003 to 0.01 (Table 2). The true binding constant for the QD–V^{2+} complex is, of course, independent of the concentration of QDs; it depends only on the change in free energy of the system upon adsorption of a ligand and the temperature of the system. The increasing values of K_a and θ_{max} upon dilution suggest that some property of the QD–ligand system that influences the binding equilibrium changes upon dilution of the QDs, and that the simple Langmuir model is unable to fully describe the QD–V^{2+} adsorption process.

Diluting the Solutions of QDs Increases the Number of Available Sites per QD. Given the observed increase in K_a and θ_{max}

with dilution of the QDs, we suspected that the mean number of available adsorption sites per QD increases as the concentration of QDs decreases. Blodt *et al.* recently reported concentration-dependent adsorption constants for water-solubilized CdSe/CdZnS/ZnS core−shell QDs and an Fe^{3+} nitrate quencher.[11] They attributed this effect to increased permeability of the ligand shell resulting from desorption of native ligands upon dilution. Importantly, observation of concentration-dependent adsorption constants in both Blodt's system and our system, which comprise different QD materials, native ligands, solvent, and quenchers, implies this effect is not system-specific. Blodt *et al.* analyzed the quenching of the QDs' PL by Fe^{3+} nitrate using the Stern−Volmer model. Here, we fit the quenching data to a Langmuir isotherm and not the Stern−Volmer model because the Stern−Volmer model does not account for the capacity of the surfaces of the QDs to accommodate multiple ligands. We hypothesized that it is the changing number of these available surface sites with concentration of the QDs that leads to the apparent concentration dependence of the quenching efficiency of V^{2+} and therefore the apparent concentration dependence of K_a.

To test this hypothesis, we first measured the PL quantum yield (QY) of a sample of QDs without added V^{2+} as a function of its concentration. Figure 3A shows that the QY of the QDs increases as they are diluted. Others have also observed this phenomenon in CdSe and ZnSe QDs.[19,20] In addition to increasing the QY of the QDs, dilution causes the band-edge transition of the QDs to shift to higher energies by 3.5 nm over the range of concentrations we explored (see Supporting Information). The QY of colloidal QDs is highly sensitive to the chemical conditions at their surfaces.[4,21] The increasing QY and blue shift of the band-edge absorption upon dilution confirms that the chemical environment at the QD surface changes upon dilution and suggests that this change may be responsible for the concentration-dependent values of K_a.

Two concentration-dependent variables that affect the local environment of the QD surfaces are (i) the degree of aggregation of the QDs and (ii) the surface coverage of the QDs with their native ligands (in this case, oleate). Others have shown that QDs can form small, solution-stable aggregates[22,23] and that aggregation of QDs causes a red shift in the band-edge absorption and a decrease in the PL intensity of the QDs.[24,25] Le Chatelier's principle dictates that diluting the QD-native ligand system will push the equilibrium of this system toward the state with the largest number of particles; that is, push the aggregation/disaggregation equilibrium toward the more disaggregated state, and push the adsorption/desorption equilibrium toward the state with more unbound oleate ligands. Disentangling the effect of ligand desorption from that of QD disaggregation on the PL of the QD and the QD−V^{2+} binding equilibrium is a major challenge and

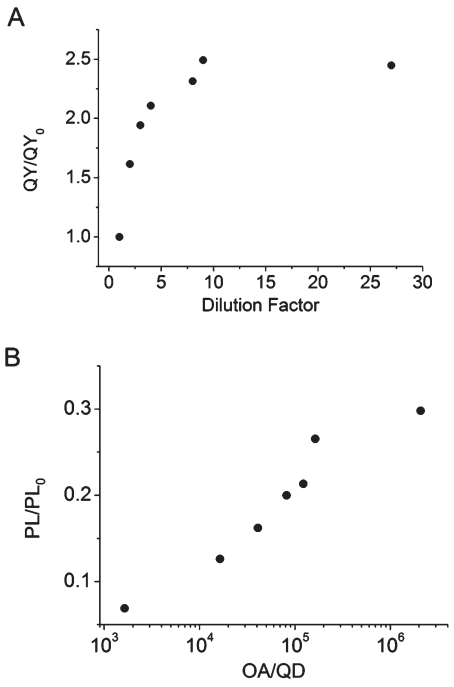

Figure 3. (A) Normalized QY of samples of CdS QDs in 40:1 $CHCl_3$/ACN as a function of their dilution factor. In this plot, the concentration of QDs with a dilution factor of 1 is 1.4×10^{-6} M. (B) Probability of finding a QD with zero adsorbed V^{2+} ligands (PL/PL_0) in solutions of 2.4×10^{-6} M V^{2+} and 4.9×10^{-8} M CdS QDs as a function of the number of oleate molecules added per QD. The value of PL_0 is given by the integrated PL intensity of a sample of 4.9×10^{-8} M CdS QDs without any added V^{2+} or oleic acid.

beyond the scope of this work. We can reasonably conclude, however, that both desorbing oleate ligands that occupy surface sites and unmasking surface area by disaggregating QDs result in an increased number of available sites to which V^{2+} can adsorb (Figure 4).

To further illustrate the competition between oleate and V^{2+} for adsorption sites on the QD, we added increasing concentrations of oleic acid to a sample of 4.9×10^{-8} M CdS QDs and 2.4×10^{-6} M V^{2+} (Figure 3B). Before addition of oleic acid, the sample had a PL/PL_0 value of 0.07; the sample was therefore nearly fully quenched. Adding oleic acid to this quenched sample caused PL/PL_0 to increase to 0.3. We interpret the recovery of PL upon addition of oleic acid as an increase in the number of QDs in the ensemble with zero adsorbed quenchers (V^{2+}) through displacement of V^{2+} by oleate. This experiment shows that V^{2+} and oleate compete for surface sites on the QD, and that increasing the surface coverage of oleate decreases the surface coverage of V^{2+}.

In order to account for the influence of oleate and QD aggregation on the V^{2+} binding equilibrium, and thereby measure a concentration-independent value of K_a for the QD−V^{2+} complex, we developed a binding model that includes an explicit description of the number of available adsorption sites per QD.

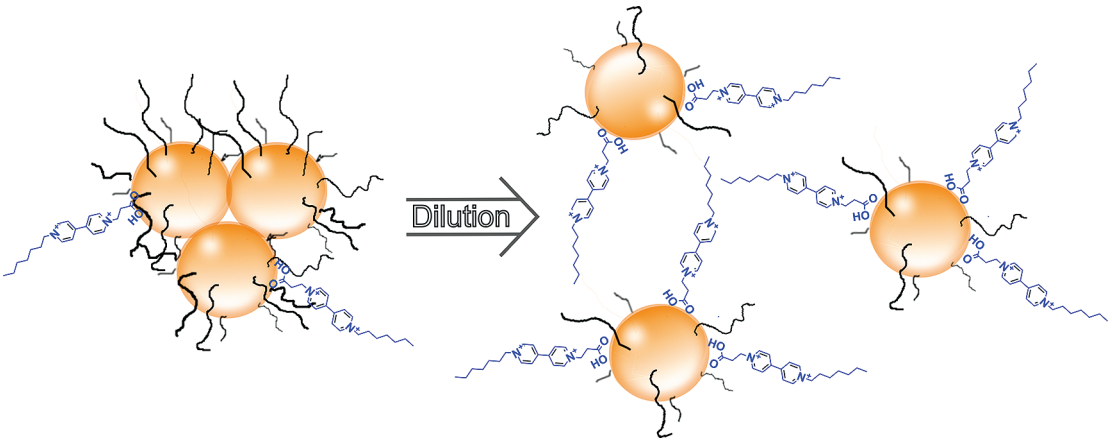

Figure 4. Illustration showing how dilution of the QD solutions can decrease the surface coverage of native ligands (drawn as black lines) and cause disaggregation of the QDs. Both of these processes result in more exposed surface area of the QD and, therefore, more available binding sites for added V^{2+}.

Derivation and Use of a Modified Langmuir Model To Account for Concentration-Dependent Surface Structure. We model the number of available sites per QD using the binomial distribution (eq 5). In eq 5, $P_{sites}(n|N,\eta)$ is the likelihood of encountering a QD

$$P_{sites}(n \mid N, \eta) = \binom{N}{n}\left(\frac{\eta}{N}\right)^{n}\left(1-\frac{\eta}{N}\right)^{N-n} \quad (5)$$

with n available surface sites, given that there are N total surface sites per QD and a mean of η available surface sites per QD in the ensemble ($\eta \leq N$). Equation 6 gives the probability of

$$P_{ligands}(m \mid n, \theta_a) = \binom{n}{m}(\theta_a)^m(1-\theta_a)^{n-m} \quad (6)$$

finding m V^{2+} bound to a QD with n available adsorption sites, where θ_a is the fractional surface coverage of available (as opposed to total) surface sites. Equation 6 is identical to eq 1 except that the total number of surface sites, N, has been replaced by the number of available surface sites, n, and the fractional surface coverage of total sites, $\theta = \langle m\rangle/N$, has been replaced by the fractional surface coverage of available sites, $\theta_a = \langle m\rangle/\eta\rangle$. The probability of finding a QD with m adsorbed V^{2+} depends on the number of available sites. Combining eq 5 and eq 6 yields the probability of finding m adsorbed V^{2+} in an ensemble of QDs with N total surface sites (eq 7).

$$P(m \mid N, \theta_a, \eta) = \sum_{n=0}^{N} P_{sites}(n \mid N, \eta)P_{ligands}(m \mid n, \theta_a) \quad (7a)$$

$$= \sum_{n=0}^{N}\left[\binom{N}{n}\left(\frac{\eta}{N}\right)^{n}\left(1-\frac{\eta}{N}\right)^{N-n}\right]\left[\binom{n}{m}{\theta_a}^m(1-\theta_a)^{n-m}\right] \quad (7b)$$

Equation 7 weights the probability of finding m adsorbed V^{2+} on a QD with n available surface sites (second term in square brackets) by the probability of finding a QD with n available surface sites (first term in square brackets), and then sums over all possible values of n ($n = 0$ to $n = N$).

Equations 8a and 8b express PL/PL_0, the probability of encountering a QD in the ensemble

$$\frac{PL}{PL_0} = P(0 \mid N, \theta_a, \eta) \quad (8a)$$

$$= \sum_{n=0}^{N}\binom{N}{n}\left(1-\frac{\eta}{N}\right)^{N-n}\left(\frac{\eta}{N}-\frac{\eta\theta_a}{N}\right)^{n} \quad (8b)$$

$$= \left(1-\frac{\eta\theta_a}{N}\right)^{N} \quad (8c)$$

with zero adsorbed V^{2+} ($m = 0$) in terms of eq 7. Applying the binomial theorem[26] to eq 8b and simplifying the result leads to eq 8c. We solved eq 8c for θ_a to obtain eq 9. We then substituted

$$\theta_a = \left(1-\left(\frac{PL}{PL_0}\right)^{1/N}\right)\frac{N}{\eta} \quad (9)$$

eq 9 into modified versions of eqs 3 and 4, where each θ is replaced by θ_a and N is replaced by η. We also omitted θ_{max} from eq 4 because the number of available surface sites per QD is included in the model as n. Solving the resulting equation for PL/PL_0 yields eq 10.

$$\frac{PL}{PL_0} = \left(\frac{1}{2[QD]K_aN}\left(2K_a[QD]N - K_a[QD]\eta - K_a[V^{2+}]_{total} - 1 + ((K_a[QD]\eta)^2 - 2K_a^2\eta[QD][V^{2+}]_{total} + 2K_a\eta[QD] + K_a^2[V^{2+}]_{total}{}^2 + 2K_a[V^{2+}]_{total} + 1)^{1/2}\right)\right)^{N} \quad (10)$$

Despite its apparent complexity, eq 10 is convenient for three reasons: (i) The experimentally observable quantity PL/PL_0 is given in terms of the total concentration of V^{2+}, which is specified when the samples are prepared, instead of the concentration of free (unbound) V^{2+}, as in the Langmuir isotherm. (ii) Equation 10 contains

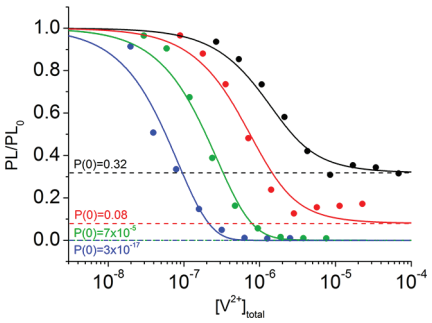

Figure 5. Probability of finding a QD with zero adsorbed V^{2+} ligands (PL/PL_0) as a function of the total concentration of V^{2+} added to the solution for samples of 1.4×10^{-6} M CdS QDs (D0, black), 4.6×10^{-7} M CdS QDs (D1, red), 1.5×10^{-7} M CdS QDs (D2, green), and 5.1×10^{-8} M CdS QDs (D3, blue). The solid lines are the best-fits using eq 10 and sharing the value of K_a across all four concentrations. We obtain a globally fit value of K_a of 8.7×10^5 M^{-1}. The dashed lines show the probability of finding QDs with zero empty surface sites as given by the value of η in eq 5. This fraction of QDs is unquenchable and, therefore, defines a lower limit for the value of PL/PL_0 for each series.

only two unknown parameters, the QD–V^{2+} adsorption constant, K_a, and the mean number of available sites per QD, η. The concentration of QDs, [QD], is easily determined from their absorption spectrum or through other analytical methods,[13,27] and we are able to estimate the total number of surface sites, N, from the surface area of the QD.[7] (iii) We can use eq 10 to globally fit the binding curves of all four concentrations of QDs simultaneously and find a single value of K_a for all of the concentrations D0–D3.

Figure 5 shows the best global fits of the plots of PL/PL_0 *versus* total concentration of V^{2+} for samples D0–D3 using eq 10; the last two columns in Table 2 list values of η and K_a obtained from these fits. When fitting the data using eq 10, we share K_a (which is independent of the number of available surface sites and, therefore, independent of concentration) between all four curves but allow each individual curve to have a unique value for η. The concentration of QDs and total number of surface sites, N, are both specified and fixed before fitting. We find that K_a for the CdS QD–V^{2+}complex is 8.7×10^5 M^{-1}. Reported values of adsorption constants for QD–ligand complexes range from 10^1 to 10^9 M^{-1} depending on the types of QD, ligand, solvent, and method of measurement.[3,5–10,28] The value that we find for CdS QDs and V^{2+} is most similar to the values found for trioctylphosphine oxide on InP QDs (3.3×10^5 M^{-1})[9,10] and thiols on CdSe QDs (4.9×10^4 M^{-1}).[8] The Supporting Information contains a table summarizing previously measured values of QD–ligand adsorption constants.

Figure 5 also shows that the PL quenching curves saturate at PL/PL_0 equal to 0.3 for D0 (black), 0.08 for D1 (red), and below the limit of detection for D2 (green) and D3 (blue). The saturation of the PL quenching curve results from the presence of "unquenchable" QDs in the ensemble; these QDs have zero available surface sites to which V^{2+} can adsorb. Once PL/PL_0 reaches the saturated value, adding more V^{2+} does not decrease the PL of the sample because all of the QDs with available surface sites have already been quenched. Equation 5 allows us to calculate the fraction of QDs with zero available surface sites ($n = 0$) for each dilution series using the values of η found by fitting the data in Figure 5. The fractions of unquenchable QDs predicted by eq 5 are indicated by the dashed lines in Figure 5. The close agreement between the predicted fraction of unquenchable QDs and the saturation of the experimentally determined PL/PL_0 in Figure 5 is strong evidence that our model accurately describes the changing number of available sites per QD upon dilution. Furthermore, the saturation of PL/PL_0 before it reaches zero confirms that the number of available sites per QD is a distributed quantity because some fraction of the sample must have zero available surface sites and is unquenchable by V^{2+}, while the remaining QDs have one or more available surface sites and are quenched upon addition of V^{2+}.

CONCLUSION

We studied the response of the PL of a solution-phase ensemble of oleate-passivated CdS QDs to addition of the PL quenching molecule V^{2+} and found that the number of surface sites available for adsorption of V^{2+} increases as the concentration of the QDs decreases (Table 2). We showed that an adsorption model that does not take into account the changing conditions at the surface of the QD with dilution yields values of K_a that depend on the concentration of QDs (Figure 2, Table 2). We developed a model that is based on the Langmuir isotherm but includes two binomial distributions: one to describe the number of available surface sites per QD and one to describe the number of adsorbed V^{2+} per QD. Fits of the PL quenching data using this model yield (i) a single value of K_a for the QD–V^{2+} complex at all concentrations of QDs and (ii) the distribution of available binding sites at each concentration (Figure 5, Table 2). Our model does not account for the possibility of V^{2+} displacing native ligands from the surface of the QD or causing the QDs to disaggregate; these inadequacies may cause the model to deviate from the PL data at concentrations of V^{2+} higher than those we can access in this system.

Understanding the relationship between the binding head group, surface structure of the QD, and interligand interactions on the binding affinity of ligands for QDs requires that we accurately measure K_a for a wide variety of QDs and ligands. Characterization of all of the surface processes (such as aggregation or disaggregation, or competing ligand equilibria) that affect the adsorption equilibrium of QD–ligand

systems remains a major challenge because of the difficulty in quantitatively characterizing the distribution of free and bound ligands in a solution-phase sample. This work shows that these processes do not need to be completely characterized in order to account for their effect on the yield of ligand exchange. The most promising strategy for determining adsorption constants of ligands and QDs within a heterogeneous mixture appears to be diffusion-ordered spectroscopy (DOSY) NMR. Hens and co-workers have recently used this method to derive diffusion coefficients for phosphonic acid and oleic acid ligands free in solution and bound to CdSe QDs.[29] These measurements, however, require concentrations of sample that are 2 orders of magnitude larger than what is appropriate for photoluminescence measurements, so it is difficult, at this point, to provide meaningful comparisons of the data from these techniques. We are currently working on building models to bridge the binding data from the two concentration regimes. Our model is potentially useful for distinguishing among various mechanisms for PL quenching (such as energy transfer, hole or electron transfer, and reorganization of passivating ligands) in the mixed-chromophore systems such as the QD-Ru-polypyridine complexes studied by Meyer, Klimov, and co-workers.[30] Knowledge of the mean and distribution of the number of ligands adsorbed per QD within an ensemble is also important in determining the intrinsic (single donor–single acceptor) electron transfer rate constant, k_{int}, for a QD–ligand system, as we discuss in our previous publication on CdS–V^{2+} complexes.[7] Importantly, however, it is this *number* of adsorbed ligands per QD (which is an experimentally measurable quantity once a distribution—Poisson or binomial—is asserted) and not the fractional surface coverage of ligands on the QD that is important for calculating k_{int} because the probability of electron transfer depends only on the number of available electron transfer pathways. The value of k_{int} we report in that publication is therefore valid. The value of K_a we report in that publication, which does depend on the fractional surface coverage, is actually a convolution of the "true" CdS–V^{2+} K_a that we derive here and the equilibrium constants for other surface processes (aggregation and native ligand adsorption) present in the system. It is therefore an effective K_a at the specific concentration of QDs at which we did the measurement.

We believe that the binding model we derive and demonstrate here will be useful in other adsorbate–substrate systems beyond QD–ligand complexes where the number of available or active sites is important but not easily measured. For example, heterogeneous catalysts often contain many types of surface sites available to target molecules, and in general, a small fraction of surface sites on the substrate are responsible for the majority of catalytic activity. These surfaces are susceptible to poisoning by molecules that irreversibly bind to the active sites.[31,32] Target molecules are often incapable of displacing these poisons from active sites, and thus poisons render the sites unavailable to adsorption by the target molecule. Our binding model could be adapted to this type of system to describe both the distribution of target molecules adsorbed to catalytically active sites and the distribution of available sites left unpoisoned.

Acknowledgment. This material is based upon work supported by the NSF under a Graduate Research Fellowship (for A.J.M.-C.), through the Northwestern Materials Research Science and Engineering Center (NU-MRSEC) Research Experience for Undergraduates program (for V.V.); by the DOE through a Computational Science Graduate Fellowship (for M.G.R., DE-FG02-97ER25308) and the Office of Science Early Career Research Award (DE-SC0003998); and by the David and Lucille Packard Foundation through a Packard Fellowship for Science and Engineering.

Supporting Information Available: Integration of PL spectrum, appearance of charge transfer emission peak in PL spectrum, comparison of binomial and Poisson distributions, dilution-induced blue shift in QD absorption spectrum, previous measurement of K_a for QD–ligand complexes. This material is available free of charge *via* the Internet at http://pubs.acs.org.

REFERENCES AND NOTES

1. Kamat, P. V. Meeting the Clean Energy Demand: Nanostructure Architectures for Solar Energy Conversion. *J. Phys. Chem. C* **2007**, *111*, 2834–2860.
2. Tagliazucchi, M.; Tice, D. B.; Sweeney, C. M.; Morris-Cohen, A. J.; Weiss, E. A. Ligand-Controlled Rates of Photoinduced Electron Transfer in Hybrid CdSe Nanocrystal/ Poly(viologen) Films. *ACS Nano* **2011**, DOI: 10.1021/nn203683s.
3. Donakowski, M. D.; Godbe, J. M.; Sknepnek, R.; Knowles, K. E.; Olvera de la Cruz, M.; Weiss, E. A. A Quantitative Description of the Binding Equilibria of *para*-Substituted Aniline Ligands and CdSe Quantum Dots. *J. Phys. Chem. C* **2010**, *114*, 22526–22534.
4. Knowles, K. E.; Tice, D. B.; McArthur, E. A.; Solomon, G. C.; Weiss, E. A. Chemical Control of the Photoluminescence of CdSe Quantum Dot–Organic Complexes with a Series of *para*-Substituted Aniline Ligands. *J. Am. Chem. Soc.* **2009**, *132*, 1041–1050.
5. Ginger, D. S.; Munro, A. M.; Jen-La Plante, I.; Ng, M. S. Quantitative Study of the Effects of Surface Ligand Concentration on CdSe Nanocrystal Photoluminescence. *J. Phys. Chem. C* **2007**, *111*, 6220–6227.
6. Ji, X.; Copenhaver, D.; Sichmeller, C.; Peng, X. Ligand Bonding and Dynamics on Colloidal Nanocrystals at Room Temperature: The Case of Alkylamines on CdSe Nanocrystals. *J. Am. Chem. Soc.* **2008**, *130*, 5726–5735.
7. Morris-Cohen, A. J.; Frederick, M. T.; Cass, L. C.; Weiss, E. A. Simultaneous Determination of the Adsorption Constant and the Photoinduced Electron Transfer Rate for a CdS Quantum Dot–Viologen Complex. *J. Am. Chem. Soc.* **2011**, *133*, 10146–10154.
8. Bullen, C.; Mulvaney, P. The Effects of Chemisorption on the Luminescence of CdSe Quantum Dots. *Langmuir* **2006**, *22*, 3007–3013.
9. Moreels, I.; Martins, J. C.; Hens, Z. Ligand Adsorption/ Desorption on Sterically Stabilized InP Colloidal Nanocrystals: Observation and Thermodynamic Analysis. *ChemPhysChem* **2006**, *7*, 1028–1031.
10. Moreels, I.; Martins, J. C.; Hens, Z. Solution NMR Techniques for Investigating Colloidal Nanocrystal Ligands: A Case Study on Trioctylphosphine Oxide at InP Quantum Dots. *Sens. Actuators, B* **2007**, *126*, 283–288.

11. Boldt, K.; Jander, S.; Hoppe, K.; Weller, H. Characterization of the Organic Ligand Shell of Semiconductor Quantum Dots by Fluorescence Quenching Experiments. *ACS Nano* **2011**, *5*, 8115–8123.
12. Yu, W. W.; Peng, X. Formation of High-Quality Cds and Other II−VI Semiconductor Nanocrystals in Noncoordinating Solvents: Tunable Reactivity of Monomers. *Angew. Chem.* **2002**, *41*, 2368–2371.
13. Yu, W. W.; Qu, L.; Guo, W.; Peng, X. Experimental Determination of the Extinction Coefficient of CdTe, CdSe, and CdS Nanocrystals. *Chem. Mater.* **2003**, *15*, 2854–2860.
14. Bittner, A. M.; Wu, X. C.; Kern, K. Synthesis, Photoluminescence, and Adsorption of CdS/Dendrimer Nanocomposites. *J. Phys. Chem. B* **2005**, *109*, 230–239.
15. Lian, T. Q.; Song, N. S.; N., H.; Zhu, H. M.; Jin, S. Y.; Zhan, W. Poisson-Distributed Electron-Transfer Dynamics from Single Quantum Dots to C_{60} Molecules. *ACS Nano* **2011**, *5*, 613–621.
16. Tachiya, M. Kinetics of Quenching of Luminescent Probes in Micellar Systems 0.2. *J. Chem. Phys.* **1982**, *76*, 340–348.
17. Tachiya, M. Application of a Generating Function to Reaction-Kinetics in Micelles: Kinetics of Quenching of Luminescent Probes in Micelles. *Chem. Phys. Lett.* **1975**, *33*, 289–292.
18. There are two solutions, but eq 10 is the only physical solution. The other solution yields negative values for PL/PL_0.
19. Xu, X.; Stöttinger, S.; Battagliarin, G.; Hinze, G.; Mugnaioli, E.; Li, C.; Müllen, K.; Basché, T. Assembly and Separation of Semiconductor Quantum Dot Dimers and Trimers. *J. Am. Chem. Soc.* **2011**, *133*, 18062–18065.
20. Mei, B. C.; Wang, J.; Qiu, Q.; Heckler, T.; Petrou, A.; Mountziaris, T. J. Dilution Effects on the Photoluminescence of ZnSe Quantum-Dot Dispersions. *Appl. Phys. Lett.* **2008**, *93*, 083114/1–083114/3.
21. Morris-Cohen, A. J.; Donakowski, M. D.; Knowles, K. E.; Weiss, E. A. The Effect of a Common Purification Procedure on the Chemical Composition of the Surfaces of CdSe Quantum Dots Synthesized with Trioctylphosphine Oxide. *J. Phys. Chem. C* **2010**, *114*, 897–906.
22. Biju, V.; Makita, Y.; Sonoda, A.; Yokoyama, H.; Baba, Y.; Ishikawa, M. Temperature-Sensitive Photoluminescence of CdSe Quantum Dot Clusters. *J. Phys. Chem. B* **2005**, *109*, 13899–13905.
23. Pal, S. K.; Narayanan, S. S. Aggregated CdS Quantum Dots: Host of Biomolecular Ligands. *J. Phys. Chem. B* **2006**, *110*, 24403–24409.
24. Mountziaris, T. J.; Mei, B. C.; Wang, J.; Qiu, Q.; Heckler, T.; Petrou, A. Dilution Effects on the Photoluminescence of ZnSe Quantum-Dot Dispersions. *Appl. Phys. Lett.* **2008**, 93.
25. Koole, R.; Liljeroth, P.; de Mello Donegá, C.; Vanmaekelbergh, D.; Meijerink, A. Electronic Coupling and Exciton Energy Transfer in CdTe Quantum-Dot Molecules. *J. Am. Chem. Soc.* **2006**, *128*, 10436–10441.
26. Brualdi, R. A. *Introductory Combinatorics*, 3rd ed.; Prentice Hall: Upper Saddle River, NJ, 1999.
27. Jasieniak, J.; Smith, L.; Embden, J. v.; Mulvaney, P.; Califano, M. Re-examination of the Size-Dependent Absorption Properties of CdSe Quantum Dots. *J. Phys. Chem. C* **2009**, *113*, 19468–19474.
28. Koole, R.; Schapotschnikow, P.; Donega, C. D.; Vlugt, T. J. H.; Meijerink, A. Time-Dependent Photoluminescence Spectroscopy as a Tool To Measure the Ligand Exchange Kinetics on a Quantum Dot Surface. *ACS Nano* **2008**, *2*, 1703–1714.
29. Gomes, R.; Hassinen, A.; Szczygiel, A.; Zhao, Q.; Vantomme, A.; Martins, J. C.; Hens, Z. Binding of Phosphonic Acids to CdSe Quantum Dots: A Solution NMR Study. *J. Phys. Chem. Lett.* **2011**, *2*, 145–152.
30. Sykora, M.; Petruska, M. A.; Alstrum-Acevedo, J.; Bezel, I.; Meyer, T. J.; Klimov, V. I. Photoinduced Charge Transfer between CdSe Nanocrystal Quantum Dots and Ru-Polypyridine Complexes. *J. Am. Chem. Soc.* **2006**, *128*, 9984–9985.
31. Hetrick, C. E.; Patcas, F.; Amiridis, M. D. Effect of Water on the Oxidation of Dichlorobenzene over V_2O_5/TiO_2 Catalysts. *Appl. Catal., B* **2011**, *101*, 622–628.
32. Jiang, B. Q.; Wu, Z. B.; Liu, Y.; Lee, S. C.; Ho, W. K. DRIFT Study of the SO_2 Effect on Low-Temperature SCR Reaction over $Fe\text{-}Mn/TiO_2$. *J. Phys. Chem. C* **2010**, *114*, 4961–4965.